Glass Temperature Effects on Probe Diffusion in Dextran Solutions†

George D. J. Phillies* and Carol Ann Quinlan

Department of Physics, Worcester Polytechnic Institute, Worcester, Massachusetts 01609

Received December 26, 1991; Revised Manuscript Received March 4, 1992

ABSTRACT: Light-scattering spectroscopy was used to measure the probe diffusion coefficient D of mesoscopic optical probes in dextran:water solutions at various temperatures. D and the solution viscosity η are fit well by modified Vogel-Fulcher-Tamman forms, e.g., $D \sim T \exp(-A/(T - T_g))$, with T_g independent of c and M. Weak yet reproducible deviations of D from Walden's rule $D \sim T/\eta$, η being the solvent viscosity, were observed, D increasing faster than expected from the temperature dependence of η. The deviations increase with increasing dextran concentration but are independent of dextran molecular weight. It was previously observed [Phillies, G. D. J.; Gong, J.; Li, L.; Rau, A.; Zhang, K.; Yu, L.-P.; Rollings, J. *J. Phys. Chem.* **1989**, *93*, 6219-6223] that these systems exhibit a stretched-exponential [$D \sim \exp(-\alpha c^{\nu})$] concentration dependence of D, with $\alpha \sim M^{0.8}$ and ν falling from 1.0 to 0.6 with increasing M, in strong support of the hydrodynamic scaling model of polymer solution dynamics. Our results reject the hypotheses that the concentration dependence of D follows from a near-exponential dependence of T_g on c or that the observed M dependence of D arises from a T dependence of intermediate variables.

Introduction

The dynamics of polymer molecules in concentrated solutions are a substantial theme in modern experimental physical chemistry. One approach to a better understanding of polymer dynamics is to study the effect of diffusant architecture—the extent to which the shape of a diffusing macromolecule affects that macromolecule's diffusion coefficient. Such studies involve solutions containing a solvent, a *probe* macromolecule whose diffusion coefficient D is measured, and a perhaps-concentrated *matrix* polymer whose effect on D is to be determined.

The probe and matrix species may be the same; however, to distinguish between consequences of probe and matrix architectures, one must confront a given probe with a series of different matrices, or vice versa. For example, Lodge et al.[1] examined diffusion of linear and star probe polymers through a matrix solution composed of linear polymer chains in a small-molecule solvent. On the other hand, work from this laboratory[2] and elsewhere[3,4] has emphasized observation of the diffusion of spherical probe particles through polymer solutions, the chain length (molecular mass M) and concentration c of the matrix polymer both being accessible to experimental variation.

There remain disagreements (e.g., see refs 1 and 5) on how D should be interpreted. It is uniformly found that D falls sharply as the concentration and molecular weight of the matrix polymer are increased. A variety of functional forms have been used to describe $D(c)$. Systematic examination finds[3,4,6,7] that the concentration dependence of D is almost always well-approximated by a stretched-exponential form

$$D = D_0 \exp(-\alpha c^{\nu}) \qquad (1)$$

even when the data under consideration was initially described by its originators in terms of some other function. Here ν is a scaling exponent, while α and D_0 are scaling prefactors.

Some authors[1] treat eq 1 as being only a convenient empirical expression. A heuristic derivation of eq 1—the "hydrodynamic scaling model"[8]—gives numerical estimates of α and ν. To our knowledge, no other model of polymer motion explicitly predicts eq 1 as a functional form, so observation of this form supports (but does not prove) the validity of the hydrodynamic scaling picture. D_0 is formally the $c \to 0$ limit of eq 1. When extensive, accurate measurements are made at low matrix concentrations, D_0 is found[9] to be somewhat larger than the dilute-solution limiting value of D, implying that eq 1 fails at very small c.

A substantial potential criticism of eq 1 is that this equation was applied to measurements made at a single absolute temperature T. It is well-known that the glass temperature T_g of a solution increases very sharply with increasing matrix c, so measurements taken at fixed T and different c have been taken at very different distances $T - T_g$ from T_g. By measurement of D at multiple temperatures and (after correction for the temperature dependence of the solvent viscosity η_s) comparison of D values taken at fixed $T - T_g$, the (hypothesized) part of the c dependence of D arising from the strong dependence of T_g on c would be removed. D at constant $T - T_g$ may be very different from D at constant T.

We have previously reported[10] extensive measurements on diffusion of polystyrene latex sphere probes in dextran:water solutions. For M as large as 5.0×10^5 Da and c as large as 250 g/L, D consistently obeys eq 1 for all polymer molecular masses and concentrations studied. In agreement with predictions of the hydrodynamic scaling model, in dextran:water solution $\alpha \sim M^{0.8}$, while (with increasing M) ν falls smoothly from 1.0 toward 0.5. These measurements were all made at 25 °C.

The objective of this paper is to reexamine probe diffusion in dextran:water solutions in light of criticisms based on the proposed behavior of T_g in these solutions. The approach used here was to measure η and D at a series of temperatures, extract any T dependence of the solvent viscosity or c dependence of T_g, and thus isolate remaining correlations between D and T.

Experimental Methods

The dextrans used here were the same as those reported[10] in our previous publication. Nominal polymer molecular masses were 10, 70, 110, and 500 kDa, the 10-, 70-, and 500-kDa materials (hereinafter samples T10, T70, and T500) being obtained from Pharmacia, while the 110-kDa sample and a second 500-kDa

† The partial support of this work by the National Science Foundation under Grant DMR90-43885 is gratefully acknowledged.

0024-9297/92/2225-3110$03.00/0

Table I
Molecular Weights of the Dextran Samples Used in This Study

sample	M_n	M_w	M_w/M_n
T10	5 450	11 800	2.17
T70	72 000	83 500	1.16
f110	69 800	121 000	1.74
f500	312 500	462 000	1.48
T500	317 000	542 000	1.71

sample (hereinafter, samples f110, f500) were obtained from Fluka AG. Characterizations of each dextran, based on determination of full molecular weight distributions as described in our previous paper[10] on these materials, appear in Table I.

Solutions were prepared using 18-MΩ conductivity water passed through a 0.1-μm microporous filter. The dextran concentrations studied here were 30, 100, 200, and in some cases 300 g/L; in the previous paper, dextran concentrations reached 250 g/L. Passage of dextran solutions through microporous filters (pore diameters of 0.22 μm or, in a few cases, 0.4 μm) was adequate to clarify all samples to a level suitable for light-scattering experiments.

Quasi-elastic light-scattering spectroscopy was used to determine the diffusion coefficient of dilute optical probe particles suspended in the dextran solutions. The methods used here have previously been described in detail,[10] so only a summary is now given. Probe particles were polystyrene latex spheres (Seradyn), carboxylate modified, with a nominal diameter of 0.067 μm. Stock sphere solutions were diluted 500:1 (v/v) into filtered dextran solutions in the final scattering cells and then mixed thoroughly. Spectra of the sphere:dextran solutions are far more intense than are the spectra of sphere-free dextran:water solutions. As shown in the previous paper,[10] scattering by the spheres dominates scattering by the dextrans, so correction of sphere spectra for scattering by the dextran is not required.

Light-scattering spectra were obtained using a 20-mW HeNe laser and optical train operated in the homodyne mode. Scattering cells were mounted in a massive copper block through which refrigerated or heated water was passed; temperature stability was better than ±0.1 K. The light scattered through 90° was analyzed using a 144 channel (128 data channels, 16 delayed (baseline) channels) digital autocorrelator. Computer control of the bath circulator and correlator permitted acquisition of complete temperature series without human intervention.

Spectra were analyzed by the method of cumulants,[11] using the baseline determined from the correlator delay channels. The measured and nominal (P^2/N) baselines agreed to within parts in 10^4 or better. Correlator sample times (bin widths) were automatically adjusted so that the 50% decay point fell between the 15th and 30th correlator channels. Signal-to-noise ratios, defined as the ratio of the cumulant-calculated amplitude at $t = 0$ to the root-mean-square scatter of the data around the best cumulant fit, were almost always in the range 300–1000.

Each spectrum was fit separately to cumulant series incorporating from one cumulant (a single exponential) to four cumulants, the probe diffusion coefficient D being obtained from the best-fit series. In almost all measurements, a two-cumulant series was adequate to describe the light-scattering spectrum, use of additional cumulants affording no significant improvement in the quality of the fit. The spectral variance V, defined as $V = 100\sqrt{K_2/K_1}$, is a measure of the deviation of the spectrum from a single-exponential form. Here K_i is the ith cumulant. V was slightly larger in dextran solutions than in pure water but did not depend significantly on temperature, dextran concentration, or dextran molecular weight.

Viscosities were measured with a series of Calibrated Ubbelohde and Cannon-Fenske (capillary) viscometers operated in a well-stirred bath. Temperature stability was provided by an external refrigerated/heated circulator with stability better than 0.1 K. Viscometer flow times were kept longer than values at which kinetic energy corrections would be significant.

Experimental Results

Representative data (and functional fits treated below) appear as Figure 1a–d. Complete viscosity measurements appear in the supplemental materials as Tables S1–S5 and Figures S1–S17. While all data needed to understand our conclusions appear in this paper, occasional references to the supplemental materials will be made to aid readers in correlating the text and supplemental pages. Measurements are presented in order of increasing molecular weight and (within each molecular weight) in order of increasing matrix concentration. In each system, η was measured at 10-deg intervals over the range 10–60 °C. Changes in c, M, and T cause the solution viscosity to be distributed over more than 3 orders of magnitude, from $\eta < 0.8$ cP to $\eta \approx 1200$ cP.

Representative diffusion coefficient measurements appear as Figures 2–5. D was determined at 1- or 5-deg intervals over the range 10–60 °C, two measurements of D being made at each T. Figures 2 and 3 show D for probe particles in dilute (30 g/L) solutions of low (11.8 kDa) and high (542 kDa) molecular mass dextrans. In both cases, D is linear in T/η_s, η_s being the solvent viscosity; a linear extrapolation of the measured D to $T/\eta_s \to 0$ finds that D vanishes to within experimental error. Probes in 30 g/L solutions of the other three dextrans show the same general behavior, namely $D \to 0$ as $T/\eta_s \to 0$. Figures 4 and 5 again plot D against T/η_s, for probes in concentrated (200 g/L) solutions of 11.8- and 462-kDa dextrans. D is still linear in T/η_s. However, if one fits the data to

$$D = A + B(T/\eta_s) \tag{2}$$

A and B being the fitting parameters, one finds that A is systemically less than 0, typically by half of the value of D at $T = 10$ °C.

The complete set of diffusion coefficient measurements appear in the supplemental material as Tables S6–S22. Measurements appear in the same order as that used in Tables S1–S5. The associated Figures S18–S34 plot D and solvent viscosity η_s as D against T/η_s.

Analysis of Viscosity Measurements

For many liquids, the temperature dependence of the viscosity η is represented accurately by the Vogel–Fulcher–Tamman equation,[12] which may be written

$$\eta = \eta_o \exp(-B/(T - T_o)) \tag{3}$$

The independent fitting parameters are η_o, B, and T_o. T_o is the nominal glass temperature. Factoring B as $B = \bar{B}T_o$ alters the algebraic form of the equation but has no effect on the accuracy of any fits.

A major theme of this paper is the temperature dependence of transport properties in solutions and in the solvent (here, water). Equation 3 was therefore fit to standard values[13] for the viscosity of pure water. Since eq 3 is not exact, η_o, B, and T_o depend slightly on the data set to which the equation is applied. We used measurements of η at 1 K intervals covering the range 10–60 °C over which we studied probe diffusion. With the specified data and our weighted nonlinear-least-squares program, one obtains $B = -508.4$, $T_o = -124.5$ K, and $\eta_o = 2.983 \times 10^{-2}$ cP with a 0.04% rms error in the fit. Use of eq 3 and these parameters does not require one to believe that H_2O actually has a glass transition at T_o (after all, T_o is well below the lowest T to which H_2O can be supercooled). Regardless of its physical validity near T_o, eq 3 remains a highly accurate empirical representation of $\eta(T)$ for the temperature range that we examined.

The viscosity of each dextran:water solution, measured as a function of temperature, was fit to eq 3 under three conditions: (i) while holding $T_o = -124.5$ K, which physically corresponds to the assumption that the nominal

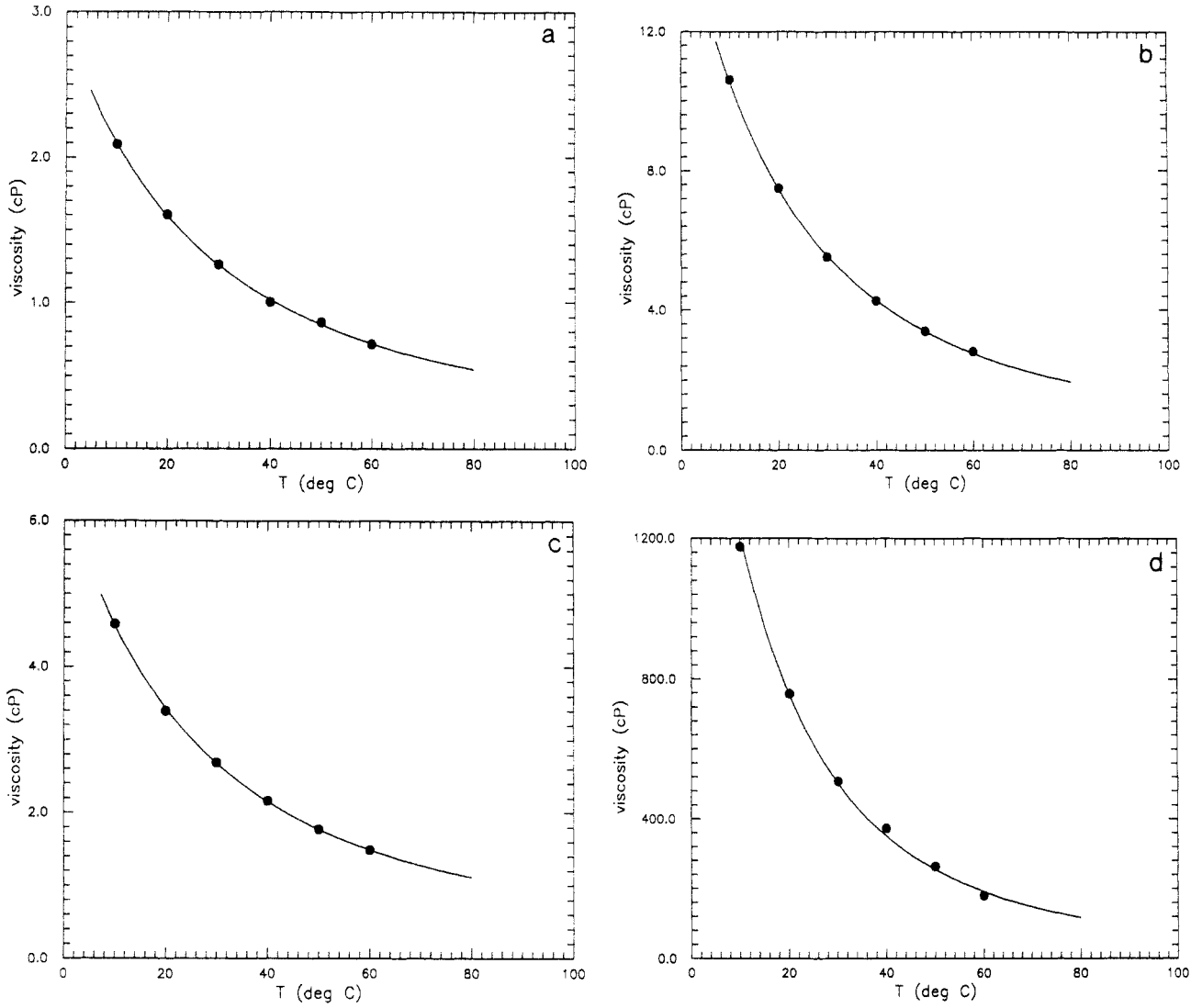

Figure 1. Viscosity of dextran:water solutions as a function of temperature and fits to Vogel–Fulcher–Tamman forms for (a) 30 g/L T10 (11.8 kDa) dextran, (b) 200 g/L T10 dextran, (c) 30 g/L T500 (542 kDa) dextran, and (d) 300 g/L T500 dextran.

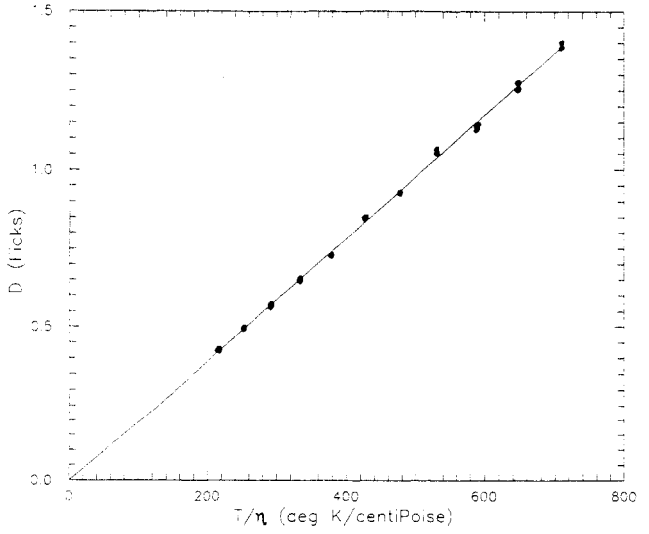

Figure 2. Diffusion coefficient of 0.067-μm polystyrene sphere probe particles in 30 g/L T10 (11.8 kDa) dextran, plotted against T/η_s, η_s being the solvent viscosity.

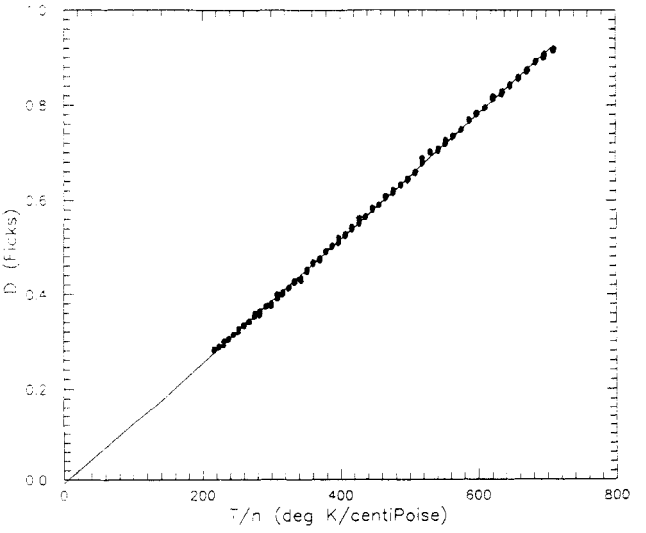

Figure 3. Diffusion coefficient of 0.067-μm polystyrene sphere probe particles in a 30 g/L solution of T500 (542 kDa) dextran, plotted against T/η_s, η_s being the solvent viscosity.

glass temperature of the solutions is the same as a nominal glass temperature of pure water, (ii) while holding T_0 = −124.5 K and B = −508.4, which physically corresponds to requiring the temperature dependence of η of each solution to be the same as the temperature dependence of the viscosity of water, and (iii) while using B, T_0, and η_0 as free parameters, which allows for the possibility that T_0 depends upon c or M.

Tables II and III summarize the utility of the Vogel–Fulcher–Tamman equation for describing η of dextran:water solutions. The complete outcomes of this analysis appear in the supplemental material, Table T1. Table II

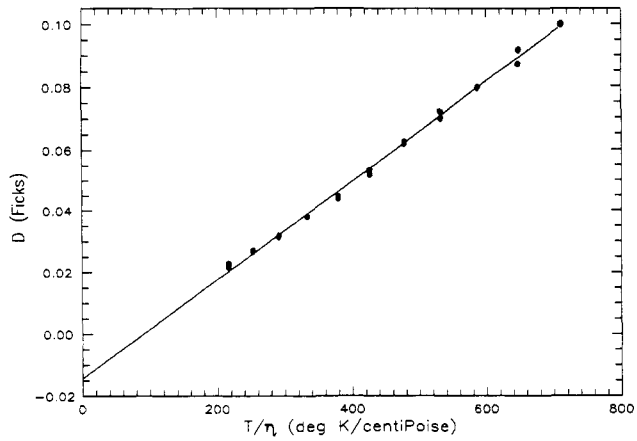

Figure 4. Diffusion coefficient of 0.067-μm polystyrene sphere probe particles in a 200 g/L solution of T70 (83.5 kDa) dextran, plotted against T/η_s, η_s being the solvent viscosity.

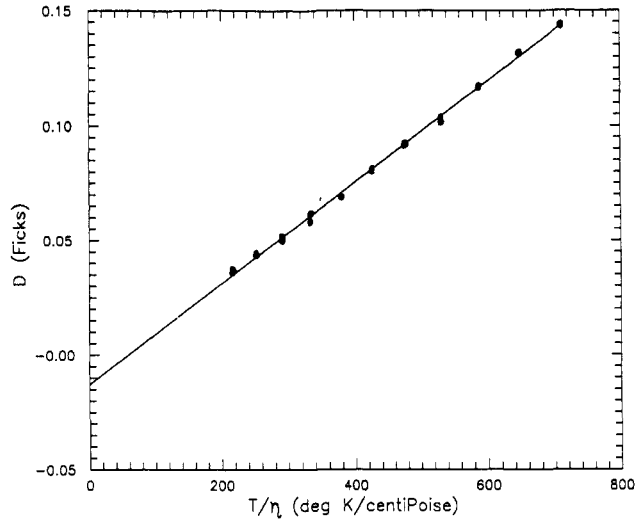

Figure 5. Diffusion coefficient of 0.067-μm polystyrene sphere probe particles in a 100 g/L solution of T500 (542 kDa) dextran, plotted against T/η_s, η_s being the solvent viscosity.

Table II
Fits to $\eta = \eta_0 \exp(-B/(T - T_0))$ for Dextran Solutions of Various Concentrations and Molecular Weights[a]

c (g/L)		T10	T70	f110	T500	f500
30	η_0	0.040	0.060	0.059	0.074	0.086
	B	−531	−536	−543	−554	−557
	% rmse	1.3	0.4	0.3	0.6	0.8
100	η_0	0.134	0.109	0.12	0.21	0.26
	B	−429	−607	−625	−671	−635
	% rmse	6.0	0.2	0.6	0.3	0.7
200	η_0	0.075	0.244	0.237	0.72	0.688
	B	−664	−723	−726	−740	−779
	% rmse	1.1	0.6	0.6	0.4	1.4
300	η_0		0.40		1.35	
	B		−827		−914	
	% rmse		0.7		4.4	

[a] T_0 was fixed at the nominal value $T_0 = -124.5$ obtained from data on pure water, while η_0 and B were retained as free parameters. % rmse is the fractional root-mean-square error in the fit, expressed as a percentage.

represents application of eq 3 with $T_0 = -124.5$ K and B a free parameter. With two exceptions (100 g/L T10 dextran, 300 g/L T500 dextran) the Vogel–Fulcher–Tamman equation with fixed $T_0 = -124.5$ K agrees with the data to within 1.4% (rms error) or better. There is no obvious trend correlating the rms error with dextran c or M. However, if T_0 is held fixed, B is found to increase substantially with increasing c, B being −530 to −560 at 30 g/L dextran, −600 to −670 at 100 g/L dextran, −660 to −780 in 200 g/L dextran, and −827 to −914 in 300 g/L dextran. At fixed c, B perhaps trends upward with increasing M, though in Table II the M dependence of B is much less pronounced than is the c dependence of B.

Table III
Fits to (i) $\eta = \eta_0 \exp(-B/(T - T_0))$ for Dextran Solutions of Various Concentrations and Molecular Weights Using T_0 and B Appropriate to Pure Water, Namely $T_0 = -124.5$ and $B = -508.4$[a]

c (g/L)	T10	T70	f110	T500	f500
30	0.04	0.05	0.07	0.10	0.10
100	−0.17	0.20	0.23	0.31	0.25
200	0.29	0.41	0.42	0.45	0.52
300		0.58		0.79	

[a] The table reports $\Delta\epsilon$, which is the fractional error [(theory − data)/data] in the few lowest-temperature points, minus the fractional error in the few highest-temperature points.

Table III describes an analysis of dextran:water viscosities against the VFT equation with T_0 and B held fixed at the values appropriate in pure water. The rms errors in these fits are typically 10–20%, far larger than the rms errors seen in Table II, in which B was a free parameter. These fits all show a strong systematic error, computed values for η having a very different temperature dependence than the experimental values have.

To characterize the systematic error, we introduce a parameter $\Delta\epsilon$, which is the fractional error [(theory − data)/data] in the few lowest-temperature points, minus the fractional error in the few highest-temperature points. $\Delta\epsilon$ gives a measure of the extent to which the fitted curve deviates from reality over the measured range of T. $\Delta\epsilon$ is a useful way to describe the systematic difference between two monotonic functions of monotonically increasing but unequal slope; with nonmonotonic functions $\Delta\epsilon$ ceases to give a useful description of the systematic error.

In Table III, $\Delta\epsilon$ increases substantially with increasing c, being roughly 5–10% with a c of 30 g/L, generally 40–50% for a c of 200 g/L, and 58–79% for a c of 300 g/L. In contrast, $\Delta\epsilon$ is the only weakly affected by the dextran molecular weight. Tables II and III are highly correlated, those data sets that yield (Table III) the most negative values of B also giving (Table III) the largest systematic differences between eq 3 and the measurements.

Finally, we match η against eq 3 while using η_0, B, and T_0 as free parameters. In almost all cases, the above mentioned fits with T_0 fixed had already had fractional rms errors at the level expected from the experimental method. Removing the constraint on T_0, so that T_0 was employed as an additional free parameter, did not improve most rms errors appreciably. Furthermore, values of T_0 from three-parameter fits were almost all within 20 deg of T_0 for pure water. Exceptions: for the T10 dextran at 100 g/L and the T500 dextran at 300 g/L, where the fits with T_0 fixed at −124.5 gave unusually large rms errors (4–6%), the three-parameter fit was a substantial improvement over the fit with T_0 constrained, at the expense of using values (−263, −726 K) for T_0 that are very different from those required at all other c and M. These two anomalies are interpreted as arising from a sensitivity of T_0 to noise in the measurements.

From Tables II and III, it is apparent that the apparent glass temperature T_0 of water:dextran solutions—as determined by a best fit of $\eta(T)$ to the Vogel–Fulcher–Tamman equation—is independent of polymer concentration and molecular mass for the concentrations ($0 \le c \le 300$ g/L) and molecular mass ($11 \le M \le 540$ kDa) that we examined. There is no evidence that the T_0 determined

Table IV
D against T for Probe Spheres in Dextran:Water as Described by the Vogel–Fulcher–Tamman Form $D = \bar{D}_0 \exp(-B/(T - T_0))$ Using Constraint Sets ii–iv Described in the Text[a]

M	c (g/L)	ii % rmse	iii B	iii % rmse	iv T_0	iv % rmse
11.8	30	1.9	509	1.2	−135	1.2
	100	1.0	575	1.0	−133	0.9
	200	2.5	635	1.6	−120	1.6
83.5	30	1.7	519	1.3	−174	1.1
	100	2.9	567	1.7	−95	1.6
	200	3.7	676	2.0	−129.5	2.0
	300	11.3	690	6.6	−82	6.5
121	30	1.3	519	0.6	−124	0.6
	100	2.8	587	1.1	−125	1.1
	200	3.7	693	3.0	−134	3.0
462	30	2.9	520	1.6	−118	1.6
	100	4.7	577	2.8	−76	2.4
	200	15	708	15	−212	12.8
542	30	2.3	518	0.8	−129	0.8
	100	4.6	605	1.6	−145	1.5
	200	5.1	721	5.0	−221	4.7
	300	20.9	669	8.0	−43	6.3

[a] M and c are the dextran molecular weight and concentration, % rmse is the root-mean-square fractional ([data − calculated]/data) error in the fit, and B and T_0 are parameters obtained while constrains iii and iv are employed, respectively. The constraints were (ii) B and T_0 from three-free-parameter fits (supplemental material, Table T1) of the VFT equation to $\eta(T)$, (iii) $T_0 = -124.5$, and (iv) no constrained parameters.

Table V
D against T for Probe Spheres in Dextran:Water as Described by a Modified Vogel–Fulcher–Tamman Form $D = \bar{D}_0(T + 273) \exp(-B/(T - T_0))$ Using Constraint Sets ii–iv Described in the Text[a]

M	c (g/L)	ii % rmse	iii B	iii % rmse	iv T_0	iv % rmse
11.8	30	1.9	509	1.2	−135	1.2
	100	1.0	575	1.0	−133	0.9
	200	2.5	635	1.6	−120	1.6
83.5	30	1.7	519	1.3	−174	1.1
	100	2.9	567	1.7	−95	1.6
	200	3.7	676	2.0	−129.5	2.0
	300	11.3	690	6.6	−82	6.5
121	30	1.3	519	0.6	−124	0.6
	100	2.8	587	1.1	−125	1.1
	200	3.7	693	3.0	−134	3.0
462	30	2.9	520	1.6	−118	1.6
	100	4.7	577	2.8	−76	2.4
	200	15	708	15	−212	12.8
542	30	2.3	518	0.8	−129	0.8
	100	4.6	605	1.6	−145	1.5
	200	5.1	721	5.0	−221	4.7
	300	20.9	669	8.0	−43	6.3

[a] M and c are the dextran molecular weight and concentration, % rmse is the root-mean-square fractional ([data − calculated]/data) error in the fit, and B and T_0 are parameters obtained while constraints iii and iv are employed respectively. The constraints were (ii) B and T_0 from three-free-parameter fits (supplemental material, Table T1) of the VFT equation to $\eta(T)$, (iii) $T_0 = -124.5$, and (iv) no constrained parameters.

from η increases appreciably at elevated dextran concentrations.

Analysis of Diffusion Measurements

To determine nominal glass temperatures from diffusion coefficients, the measured D as a function of T for each solution was fit via weighted nonlinear least-squares routine to a Vogel–Fulcher–Tamman equation

$$D = \bar{D}_0 \exp(-B/(T - T_0)) \tag{4}$$

and also to a VFT equation modified by analogy with Walden's rule $D \sim T/\eta$, namely

$$D = \bar{D}_0 T \exp(-B/(T - T_0)) \tag{5}$$

Table IV indicates outcomes from fits of the conventional VFT equation to D in solutions of various c and M. (The full set of fits appear in supplementary Table T2). Because $D \sim 1/\eta$, the sign of B reverses between fits to η and fits to D. Measurements on each solution were analyzed under four sets of constrains, viz. (i) $B = 508.43$ and $T_0 = -124.54$ K (parameters giving a best fit for pure water) with $\bar{D}_0$ as the free parameter, (ii) B and T_0 taken from the best three-free-parameter fits of eq 3 to the solution viscosity with $\bar{D}_0$ as the free parameter, (iii) $T_0 = -124.54$ K (parameter giving a best fit with pure water) with B and $\bar{D}_0$ free, and (iv) best fit with $\bar{D}_0$, B, and T_0 all free parameters.

Fits to eq 4 using constraint set i are uniformly unsatisfactory. At concentrations of 30, 100, 200, and 300 g/L, % rms errors in the fits were roughly 5, 10, 16, and 20%, respectively. The systematic errors $\Delta\epsilon$ increased progressively with increasing c, being roughly 16, 30, 40, and 50% at the four concentrations studied. There was no significant dependence of the rms error or $\Delta\epsilon$ on polymer molecular weight. Interestingly, as shown below, D is linear in T/η_s, η_s being the viscosity of pure water; however, in dextran solutions D does not extrapolate to 0 if the limit $T/\eta_s \to 0$ is taken, explaining the failure of constraint set i to reproduce the data.

Fits to eq 4 using constraint set ii (parameters from the solution viscosity) are almost always far better than fits based on set i. In most cases, fits to eq 4 had rms errors of 3–4% and a $\Delta\epsilon$ of 6–12%. However, at 200 g/L T70, T500, and f500 dextran and 300 g/L T500 dextran, the fit is significantly worse (8–16% rms error, $\Delta\epsilon \sim$ 15–35%). Furthermore, in all three of these solutions, a three-parameter ($\bar{D}_0$, B, T_0) fit to D to eq 4 does not give a good (rms error below 5%) description of the temperature dependence of D. That is, if eq 4 and constraint set ii describe D poorly, D simply is not described well by eq 4. Finally, as noted above, η of the 100 g/L solution of T10 dextran is ill-fit by eq 3 and T_0 of pure water; the parameters that describe η of this solution describe D rather poorly, an anomaly not repeated at other c or M.

Constraint sets iii (T_0 held to its value in pure water) and iv (all parameters free) are almost always equally good at describing the temperature dependence of D. For probes in solutions of the T10, T70, and f110 dextrans, rms errors in the two fits were always within a few tenths of a percent, while $\Delta\epsilon$ was insignificant (less than 3%). For the f500 and T500 dextrans, the fits were sometimes significantly worse (up to 7.7% rms error in 300 g/L T500 dextran, 15 ± 1% rms error in 200 g/L f500 dextran). However, constraint sets iii and iv both give results much better than does set i or ii. Constraining T_0 to its value in pure water, rather than letting T_0 be a free parameter, has almost no effect on the accuracy or systematic error in the fit. T_0, as determined from D, does not appear to depend on c or M.

Measurements of D in each solution were also fit to the modified Vogel–Fulcher–Tamman equation, eq 5, using the same four sets of constraints that were applied to eq 4. Key findings appear in Table V; full results of these fits appear in supplemental Table T3. The relative quality of the constraints has the same order with both equations, constraint set i giving fits consistently worse (rms errors of 10 ± 5%) than set (ii) (rms errors almost always ≤6%). Constraint set ii in turn gives fits considerably worse than set iii or iv. Constraint sets iii and iv are equally good,

Table VI
Fits to (i) $D = A_0 + A_1(T/\eta)$, η Being the Viscosity of Pure Water[a]

M (kDa)	c (g/L)	A_0	A_1	rmse
	0	1.38×10^{-2}	2.14×10^{-3}	7.8×10^{-3}
11.8	30	-1.29×10^{-3}	1.96×10^{-3}	1.09×10^{-2}
	100	-4.89×10^{-2}	1.16×10^{-3}	1.09×10^{-2}
	200	-3.60×10^{-2}	5.08×10^{-4}	0.28×10^{-2}
83.5	30	-1.41×10^{-2}	1.43×10^{-3}	0.62×10^{-2}
	100	-1.60×10^{-2}	4.84×10^{-4}	0.29×10^{-2}
	200	-1.43×10^{-2}	1.60×10^{-4}	1.33×10^{-3}
	300	-3.47×10^{-3}	4.08×10^{-5}	0.77×10^{-3}
121	30	-1.04×10^{-2}	1.36×10^{-3}	0.41×10^{-2}
	100	-2.27×10^{-2}	4.69×10^{-4}	0.25×10^{-2}
	200	-1.27×10^{-2}	1.42×10^{-4}	0.20×10^{-2}
462	30	-6.23×10^{-3}	1.00×10^{-3}	0.23×10^{-2}
	100	-7.18×10^{-3}	2.04×10^{-4}	0.23×10^{-2}
	200	-6.02×10^{-5}	2.60×10^{-5}	2.84×10^{-3}
542	30	-0.829×10^{-2}	1.31×10^{-3}	0.43×10^{-2}
	100	-1.29×10^{-2}	2.20×10^{-4}	1.39×10^{-3}
	200	-5.42×10^{-3}	4.41×10^{-5}	1.11×10^{-3}
	300	-7.15×10^{-4}	1.10×10^{-5}	3.56×10^{-4}

[a] M and c are the polymer molecular weight and concentration. rmse is the root-mean-square error in the fit; its units are the same as those of D, namely $cm^2\ s^{-1}$. A concentration c of 0 refers to a system containing no dextran, i.e. probes in pure water.

giving rms errors that are almost always in the range 1–2% and $\Delta\epsilon$ values that are almost always less than 3%.

Does eq 5 describe our results more closely than eq 4? For constraint sets iii and iv, which follow the data at the level expected from the random noise in the original light-scattering spectra, there is basically no difference in accuracy between eqs 4 and 5. Constraint set i (parameters taken from pure water) does work better (rms errors typically five percentage points less) with eq 5 than with eq 4, but with either equation there are substantial systematic differences between the analytic form and the experimental results.

To summarize, measurements of D at various T were compared with the VFT equation and an obvious modification, finding good agreement with T_0 as a free parameter and equally good agreement with T_0 constrained to be a constant, namely a nominal glass temperature of the solvent. Replacing a constrained T_0 with a T_0 that is a free parameter does not improve the rms difference between the VFT function and the observed D. Measurements of probe diffusion are therefore entirely consistent with the hypothesis that the apparent glass temperature (as obtained by applying the VFT function to probe diffusion measurements) of water:dextran solutions is independent of dextran concentration and molecular weight.

Solvent Viscosity Effects

Table VI and supplemental material Table T4 compare measurements of probe diffusion with the temperature dependence of the solvent viscosity η_s. The comparison is based on linear least-squares fits to a generalized Walden's rule

$$D = A_0 + A_1(T/\eta_s) + A_2(T/\eta_s)^2 \quad (6)$$

Here T is the absolute temperature; the A_i are fitting parameters. For each data set (fixed c and M, variable T), fits were made with (i) $A_2 = 0$ (simple linear form), (ii) $A_0 = A_2 = 0$ (Walden's rule; a linear form forced through the origin), (iii) all parameters free (full quadratic form), and (iv) $A_0 = 0$ (a quadratic forced to pass through the origin). Table VI gives results from constraint set i; Table T4 shows all parameters from all fits.

It is consistently found that D is linear in T/η_s, as seen in Figures 2–5. However, in the low-temperature ($T/\eta_s \to 0$) limit and elevated c, D does not always vanish. For c of 30 g/L, the measured A_0 is not experimentally distinguishable (less than twice the rms error) from $A_0 = 0$. At larger dextran concentrations, A_0 is substantially negative, its magnitude almost always being in the range 5–10 times the rms scatter of the data points around the best-fit straight line. In our units, A_0/A_1 is typically −50 for a c of 100 g/L and typically −100 for a c of 200 or 300 g/L. There is thus a slight tendency for the negative intercept to become more apparent at higher concentrations.

Walden's rule $D \sim T/\eta_s$, which corresponds to constraint set ii, requires A_0 and A_2 to be experimentally indistinguishable from zero. This requirement is not satisfied here. In almost every case, fits made using constraint set ii were worse than fits made using the other three constraint sets. Constraint sets i, ii, and iv gave approximately equally good descriptions of D. The full quadratic form (case iii) gave results that were no better than fits made using the simple linear form $D = A_0 + A_1(T/\eta_s)$. From Occam's rule, the full quadratic form is therefore inferior to the simple linear form or to the zero-intercept quadratic form $D = A_1(T/\eta_s) + A_2(T/\eta_s)^2$, because the latter forms have fewer parameters but give equally good fits. There appears to be no argument that forces a choice between constraint sets i and iv.

The observed failure of Walden's rule in water:dextran solutions is implicit in comparisons of η_s, η, and D with the Vogel–Fulcher–Tamman equation. η_s follows the VFT equation accurately, so if Walden's rule were satisfied, the temperature dependence of D would necessarily follow the modified VFT equation, eq 5, using B and T_0 obtained from $\eta_s(T)$ of pure water. Experimentally, η_s and D are consistent with the same value of $T_0 = -124.5$ K of pure water if B is a free parameter. Best-fit values of B obtained from D(T) differ systematically from the $B = 508.4$ that describes $\eta_s(T)$.

In water:dextran solutions, D does not scale with temperature exactly as T/η_s. Similarly, since η and η_s only agree with the VFT equation if different values of B are used, η and η_s have different dependences on temperature. The differences between η_s, and η, and D depend on the dextran concentration: they increase at large c. However (except perhaps for T10 dextran) the relative behaviors of η_s, η, and D are the same at all polymer molecular weights.

Conclusions

Phillies et al.[10] previously reported on the diffusion of probe spheres through dextran:water solutions, finding for each dextran species that

$$D = D_0 \exp(-\alpha c^{\nu}) \quad (7)$$

By comparing probes in dextrans of various molecular weights, it was shown that $\alpha \sim M^{0.8}$ and that ν falls from 1.0 to 0.6 as M increases from 11.8 to 542 kDa. These correlations of α and ν with M are precisely those predicted by the hydrodynamic scaling model,[5,8] so ref 10 concluded that its experimental results on water:dextran solutions supported hydrodynamic scaling.

From the above, D/T is not simply proportional to η_s^{-1}. With increasing T, D increases faster than η_s^{-1} does. To within experimental error, one could say that D is linear in T/η_s but that the $T/\eta_s \to 0$ intercept A_0 is negative. One could equally well say that $D \to 0$ at small T/η_s but that, at elevated T, D includes a weak positive quadratic dependence on T/η_s.

The failure of Walden's rule is very weak; fits to eq 6 with $A_0 = A_2 = 0$ forced have only twice the rms error of fits in which A_0 and/or A_2 are taken as adjustable parameters. The extent of the failure of Walden's rule is weakly c-dependent, becoming larger at elevated c. The failure is independent of polymer M. The observed correlations between D and T are all consistent with a weak variation in solvent quality with T and c. A decrease in solvent quality with increasing T would cause polymer chains to shrink at high T, thereby reducing solution microviscosity and increasing D more rapidly than expected from the decrease in η_s with increasing T. Furthermore, polymer solutions tend toward θ-like behavior as their concentration is increased. A cooperative interaction between temperature and concentration effects would lead to an increase in the failure of Walden's rule at elevated c, as observed.

The approximate dependence of D on T/η_s is consistent with a variety of models of polymer dynamics. For example, many tube-type models endow polymer beads with a bare diffusion coefficient D_e determined by solvent interactions; chain connectivity and chain crossing constraints then convert D_e into a chain self-diffusion coefficient D. D_e and hence D are reasonably expected to scale as T/η_s, so eq 6 does not serve to distinguish between hydrodynamic scaling and tube-type models. Careful examination of $D(T)$ might, however, serve to test free-volume pictures of polymer dynamics, a theme not pursued further here.

The negative intercepts seen in fits of D to $D = A_0 + A_1(T/\eta_s)$ bring to mind similar intercepts seen a decade ago[14,15] in studies of rotational diffusion coefficients D_r of small molecules in simple liquids. Then and now, the diffusion coefficient was apparently linear in T/η_s. The dependence of D_r on T/η_s was too strong, so that in the low-temperature ($T/\eta_s \rightarrow 0$) limit D_r extrapolated to a negative value. Here the behavior was described by differences between the VFT B parameters for η_s and D; a VFT-type analysis was not reportd for D_r.

It could be argued that a stretched-exponential relationship between c and D is observed because D was measured at fixed T rather than fixed distance $T - T_g$ from a glass temperature T_g, T_g being argued to be strongly correlated with c. This hypothesis was here examined by fitting η to the VFT equation and by fitting D to a modified VFT equation, thereby determining an apparent glass temperature T_0 and its dependences on c and M. For D and η, T_0 was found to be constant to within experimental error. If T_0 of the VFT equation is identified with the apparent glass temperature of these solutions, then T_g is virtually constant. Measurements of D made at constant T are therefore also made at constant $T - T_0$, so correction of D to fixed $T - T_g$ will not affect the previous[10] paper's conclusions.

Observation of the stretched-exponential form $D = D_0 \exp(-\alpha c^{\nu})$ in water:dextran solutions provides support for the hydrodynamic scaling model[5,8] because one observes the expected molecular weight dependences $\alpha \sim M^{0.8}$ and $\nu \in (1 \rightarrow {}^1/_2)$ of the scaling parameters. The disagreements with Walden's rule are independent of the polymer molecular weight, so no correction to the measured D based on Walden's rule can change the observed correlations between D and M or between α, ν, and M. The agreement of α and ν with the hydrodynamic scaling model is therefore not an artifact arising from a failure of Walden's rule (solvent-viscosity scaling) for D of probes in dextran:water solutions.

Similarly, comparison with the VFT equation finds for our relatively dilute polymer solutions that T_g is nearly constant, so correction of D to fixed $T - T_g$ rather than fixed T would not change the observed correlations between D and M or between α, ν, and M. The agreement of α and ν with the hydrodynamic scaling model is therefore not an artifact arising from hypothesized variations in T_g.

In conclusion, we have made an extensive study of the temperature dependence of probe diffusion in dextran:water solutions. D does not simply trace the solvent viscosity. Results here are consistent with our previous study of this system.[10] Previously-reported successful tests[10] of the hydrodynamic scaling model of polymer solution dynamics did not come to an erroneously favorable conclusion because the measurements were made at fixed T.

Supplementary Material Available: Tables and plots of η and ρ for dextran:water, tables and plots of D of 67-nm polystyrene latex spheres in water and dextran:water plotted against T/η_s, tables of fits of η and D to the Vogel–Fulcher–Tamman form and of D to the form $D = A_0 + A_1(T/\eta_s) + A_2(T/\eta_s)^2$ (84 pages). Ordering information is given on any current masthead page.

References and Notes

(1) Lodge, T. P.; Markland, P.; Wheeler, L. M. *Macromolecules* **1989**, *22*, 3409.
(2) Phillies, G. D. J.; Pirnat, T.; Kiss, M.; Teasdale, N.; Maclung, D.; Inglefield, H.; Malone, C.; Rau, A.; Yu, L.-P.; Rollings, J. *Macromolecules* **1989**, *22*, 4068.
(3) Russo, P. S.; Mustafa, M.; Cao, T.; Stephens, L. K. *J. Colloid Interface Sci.* **1988**, *122*, 120.
(4) Brown, W.; Rymden, R. *Macromolecules* **1986**, *19*, 2942.
(5) Phillies, G. D. J. *Macromolecules* **1990**, *23*, 2748.
(6) Phillies, G. D. J.; Ullmann, G. S.; Ullmann, K.; Lin, T.-H. *J. Chem. Phys.* **1985**, *82*, 5242.
(7) Phillies, G. D. J. *Macromolecules* **1986**, *19*, 2367.
(8) Phillies, G. D. J. *Macromolecules* **1987**, *20*, 558; **1988**, *21*, 3101.
(9) Wheeler, L. M.; Lodge, T. P. *Macromolecules* **1989**, *22*, 3399.
(10) Phillies, G. D. J.; Gong, J.; Li, L.; Rau, A.; Zhang, K.; Yu, L.-P.; Rollings, J. *J. Phys. Chem.* **1989**, *93*, 6219.
(11) Koppel, D. E. *J. Chem. Phys.* **1972**, *57*, 4814.
(12) Vogel, H. *Phys. Z.* **1921**, *22*, 645. Fulcher, G. S. *J. Am. Ceram. Soc.* **1925**, *77*, 3701. Tamman, G.; Hesse, W. *Z. Anorg. Allg. Chem.* **1926**, *156*, 245.
(13) *Handbook of Chemistry and Physics*, 44th ed.; Hodgman, C. D., Ed.; citing Bingham and Jackson, *Bulletin Bureau Standards* 14, 75 (1918).
(14) Phillies, G. D. J.; Kivelson, D. *J. Chem. Phys.* **1979**, *71*, 2575.
(15) Bauer, D. R.; Alms, G. R.; Brauman, J. I.; Pecora, R. *J. Chem. Phys.* **1974**, *61*, 2255.